Dissolution of Nonspherical Powders

NOBUYUKI KITAMORI [x] **and KATSUMI IGA**

Received December 8, 1977, from the *Pharmaceutical Research Laboratories, Central Research Division, Takeda Chemical Industries, Ltd., Yodogawa-ku, Osaka 532, Japan.* Accepted for publication March 29, 1978.

Abstract □ To elucidate the effect of particle shape on the dissolution profile of a powder, an equation was derived for the dissolution of powders whose particles are rectangular parallelepipeds and log-normally distributed by introducing three-dimensional parameters instead of diameter in the Brooke equation for the spherical powder dissolution. By using some hypothetical values for constants in the equation, it is shown that the smallest side length, a_0, does greatly affect the dissolution profile but that the other two side lengths, αa_0 and βa_0, do not, even with rather large values of α and β. Nonisotropic dissolution also is discussed.

Keyphrases □ Dissolution profiles—nonspherical powders, effect of particle shape, equations derived □ Powders, nonspherical—dissolution profiles, effect of particle shape, equations derived

Theoretical considerations of drug dissolution in relation to particle-size distribution were first presented by Higuchi and Hiestand (1, 2). Recently, Brooke (3, 4) and Pedersen and Brown (5) developed more exact equations that permit the calculation of the dissolution rate of spherical particles obeying the log-normal distribution law. Most dissolution theories describing the particle-size distribution effect considered spherical particles.

Little attention has been given to the influence of shape factors on dissolution, except that Carstensen and Patel (6) reported the dissolution of nonspherical particles of a log-normal distribution. The dissolution of nonspherical single particles was approximated by the dissolution equation for a hypothetical spherical particle of a specified diameter by Pedersen and Brown (7).

The purpose of this paper is to elucidate the effect of particle shape on dissolution profiles. An equation was derived for the dissolution of powders whose particles are rectangular parallelepipeds and log-normally distributed by introducing three-dimensional parameters instead of diameter into the Brooke equation for the spherical powder dissolution. The shape effect in cubes, needles, and plates was examined on the basis of this theory. Nonisotropic dissolution is also discussed.

THEORETICAL

For a powder whose particles are rectangular parallelepipeds and log-normally distributed, it is assumed that the side lengths of a particle initially are a_0, αa_0, and βa_0 on the edges, where α and β are constants larger than unity. Its initial volume is then $\alpha\beta a_0^3$ ($= V_0$). If it dissolves isotropically under sink conditions, then its volume after t can be written:

$$V_t = [a_0 - (2k_i/p)t][\alpha a_0 - (2k_i/p)t][\beta a_0 - (2k_i/p)t] \quad \text{(Eq. 1)}$$

where k_i is the intrinsic dissolution rate constant and p is the density. After $t = a_0 p/2k_i$, the particle volume is zero ($V_t = 0$). A log-normal particle-size distribution is given by:

$$f = \frac{1}{\sigma\sqrt{2\pi}} \exp[-(\ln M - \ln a_0)^2/2\sigma^2] \quad \text{(Eq. 2)}$$

where $\ln M$ is the logarithmic mean of a_0 and σ is the standard deviation. The weight undissolved after t is given by:

$$W_t = \int_{\ln[(2k_i/p)t]}^{\infty} pV_t N_0 f \, d(\ln a_0) \quad \text{(Eq. 3)}$$

After inserting Eq. 1 into Eq. 3 by expanding the cubic term and letting $\alpha\beta p N_0 = r$ and $(2k_i/p)t = \tau$, Eq. 3 becomes:

$$W_\tau = r\int_{\ln\tau}^{\infty} a_0^3 f \, d(\ln a_0) - \left(1 + \frac{1}{\alpha} + \frac{1}{\beta}\right) r\tau \int_{\ln\tau}^{\infty} a_0^2 f \, d(\ln a_0) + \left(\frac{1}{\alpha} + \frac{1}{\beta} + \frac{1}{\alpha\beta}\right) r\tau^2 \int_{\ln\tau}^{\infty} a_0 f \, d(\ln a_0) - \frac{1}{\alpha\beta} r\tau^3 \int_{\ln\tau}^{\infty} f \, d(\ln a_0) \quad \text{(Eq. 4)}$$

By employing a standard normal distribution function $F(x)$, as was done by Brooke (3, 4) for spherical particles, Eq. 4 becomes:

$$W_\tau = r\exp[3(\ln M + 3\sigma^2/2)]\left(1 - F\left[\frac{\ln(\tau/M) - 3\sigma^2}{\sigma}\right]\right) - \left(1 + \frac{1}{\alpha} + \frac{1}{\beta}\right) r\tau \exp[2(\ln M + \sigma^2)]\left(1 - F\left[\frac{\ln(\tau/M) - 2\sigma^2}{\sigma}\right]\right) + \left(\frac{1}{\alpha} + \frac{1}{\beta} + \frac{1}{\alpha\beta}\right) r\tau^2 \exp(\ln M + \sigma^2/2)\left(1 - F\left[\frac{\ln(\tau/M) - \sigma^2}{\sigma}\right]\right) - \frac{1}{\alpha\beta} r\tau^3 \left(1 - F\left[\frac{\ln(\tau/M)}{\sigma}\right]\right) \quad \text{(Eq. 5)}$$

The initial weight of the particles, W_0, is:

$$W_0 = r\exp[3(\ln M + 3\sigma^2/2)] \quad \text{(Eq. 6)}$$

Then the weight fraction dissolved, $S_\tau (= 1 - W_\tau/W_0)$, can be written:

$$S_\tau = F\left[\frac{\ln(\tau/M) - 3\sigma^2}{\sigma}\right] + \left(1 + \frac{1}{\alpha} + \frac{1}{\beta}\right)(\tau/M)\exp(-5\sigma^2/2)\left(1 - F\left[\frac{\ln(\tau/M) - 2\sigma^2}{\sigma}\right]\right) - \left(\frac{1}{\alpha} + \frac{1}{\beta} + \frac{1}{\alpha\beta}\right)(\tau/M)^2\exp(-4\sigma^2)\left(1 - F\left[\frac{\ln(\tau/M) - \sigma^2}{\sigma}\right]\right) + \frac{1}{\alpha\beta}(\tau/M)^3\exp(-9\sigma^2/2)\left(1 - F\left[\frac{\ln(\tau/M)}{\sigma}\right]\right) \quad \text{(Eq. 7)}$$

RESULTS AND DISCUSSION

In the dissolution equation for a powder consisting of rectangular parallelepipeds, three-dimensional parameters (a_0, α, and β) were introduced instead of diameter. Brooke (3, 4), in his equation for spherical powders, showed that the expression of the weight fraction undissolved, W_τ/W_0, is a function of only τ/M when σ is constant. Similarly, for rectangular parallelepipeds, W_τ/W_0 is dependent only on the ratio of time length to mean side length when α, β, and σ are constant.

In this paper, S_τ in Eq. 6 was calculated with a computer, using hypothetical values of these parameters, where the standard normal function $F(x)$ was approximated (8) by:

$$F(x) = 1 - \frac{1}{\sqrt{2\pi}}\exp(-x^2/2)(ay + by^2 + cy^3 + dy^4 + ey^5) \quad \text{(Eq. 8)}$$

where $y = 1/(1 + 0.2316419x)$, $a = 0.319381530$, $b = -0.356563782$, $c = 1.781477937$, $d = -1.821255978$, and $e = 1.330274429$.

Exactly calculated dissolution profiles for the hypothetical powders consisting of cubes, needles, and plates with isotropic behavior are presented in Table I as weight percent dissolved *versus* t. The parameters are based on $k_i = 0.1$, $M = 1.0$, $p = 1.5$, and $\sigma = 0$–0.7. Figure 1 shows the dissolution profiles when $\sigma = 0.5$ in Table I. In this figure, curve a is for cubes ($1 \times 1 \times 1$ on the edges; *i.e.*, $\alpha = 1.0$ and $\beta = 1.0$), curve b is for needles ($1 \times 1 \times 10$ on the edges; *i.e.*, $\alpha = 1.0$ and $\beta = 10.0$), curve c is for plates ($1 \times 10 \times 10$ on the edges; *i.e.*, $\alpha = 10.0$ and $\beta = 10.0$), and curve d is for cubes 10 times larger in size than the cubes in curve a. The ratio of the time necessary for 50% dissolution is 1:1.36:2.11:10 for the profiles.

0022-3549/78/1200-1674$01.00/0

Table I—Exactly Calculated Isotropic Dissolution Profiles for the Powders Consisting of Cubes, Needles, and Plates [a] (M = 1.0, p = 1.5, and k_i = 0.1)

Time	Cube (α = 1.0, β = 1.0)					Needle (α = 1.0, β = 10.0)					Plate (α = 10.0, β = 10.0)				
	$\sigma = 0$ [b]	0.1	0.3	0.5	0.7	0 [b]	0.1	0.3	0.5	0.7	0 [b]	0.1	0.3	0.5	0.7
1.0	34.90	34.11	28.38	19.53	11.03	25.89	25.28	20.89	14.21	7.93	15.63	15.53	12.52	8.43	4.65
2.0	60.56	59.34	50.26	35.59	20.70	47.66	46.60	38.89	26.90	15.27	30.53	30.34	24.52	16.58	9.19
3.0	78.40	77.04	66.60	48.65	29.19	65.44	64.09	54.11	38.11	22.04	44.70	44.44	36.03	24.47	13.63
4.0	89.84	88.56	78.35	59.16	36.64	79.38	77.89	66.63	47.90	28.27	58.18	57.84	47.03	32.07	17.95
5.0	96.30	95.28	86.43	67.56	43.17	89.63	88.13	76.59	56.35	33.99	70.96	70.55	57.46	39.33	22.15
10.0	99.99	99.99	99.09	89.55	6.590	99.99	99.99	97.52	82.63	55.99	99.99	99.99	91.95	68.43	40.84
15.0			99.99	96.40	78.50			99.82	93.08	70.00			99.19	84.80	55.39
20.0				98.66	85.87			99.99	97.13	79.05			99.93	92.78	66.28
30.0				99.77	93.30				99.43	89.12			99.99	98.28	80.26
60.0				99.99	98.85				99.99	97.80				99.99	95.09

[a] The values in the table are percent dissolved. [b] Since Eq. 7 does not hold for σ = 0, the dissolution profiles for monosized powders were calculated at σ = 0.0001.

Figure 1 reveals that the increase in the smallest side length, a_0, greatly affects the dissolution profiles, whereas the influence of the other two side lengths, αa_0 and βa_0, on dissolution is not severe, even with rather large values of α and β. Thus, rough evaluation of the dissolution for the powders consisting of rectangular parallelepipeds using Eq. 7 is possible, even though the particles in the powder are not exactly similar in shape.

Several investigators (1–5) approximated particles as spheres in their theories. On the other hand, by letting α and β be unity (the condition for cubes), Eq. 6 reduces to the one equation for spherical powders. This finding shows that the weight fraction dissolved for spherical powders having mean diameter M is equal to that for cubic powders having mean side length M.

The comparison of the dissolution profile for powder of acicular particles (1 × 1 × 10 on the edges) with the dissolution profiles of hypothetical spherical particles having the same volume or surface area with

Table II—Exactly Calculated Isotopic Dissolution Profiles for the Powders Consisting of Rectangular Parallelepipeds (1 × 1 × 10 on the Edges) and the Spheres Having the Same Volume or Surface Area [a] (σ = 0.5, p = 1.5, and k_i = 0.1)

Time	Rectangular Parallelepipeds (M = 1.0)	Hypothetical Spheres Having Same Volume (M = 2.673)	Hypothetical Spheres Having Same Surface Area (M = 3.656)
1.0	14.21	7.74	5.71
2.0	26.90	14.95	11.14
3.0	38.11	21.67	16.29
4.0	47.90	27.90	21.18
5.0	56.35	33.69	25.81
10.0	82.63	56.66	45.45
15.0	93.08	71.82	60.11
20.0	97.13	81.63	70.88
30.0	99.99	92.01	84.40
60.0		99.15	97.30

[a] The values in the table are percent dissolved.

Table III—Exactly Calculated Dissolution Profiles for the Powders Consisting of Rectangular Parallelepipeds (1 × 1 × 10 on the Edges) with Three Dissolution Rate Constants Proportional to the Corresponding Side Lengths and with the Average Dissolution Rate Constant k_{ia} [a] (M = 1.0, σ = 0.5, p = 1.5, α = 1.0, and β = 10.0)

Time	Nonisotropic Dissolution (k_i = 0.1, 0.1, 10.0)	Isotropic Dissolution (k_{ia} = 0.14286)
1.0	19.53	19.83
2.0	35.59	36.59
3.0	48.65	50.45
4.0	59.16	61.63
5.0	67.56	70.46
10.0	89.55	92.12
15.0	96.40	97.75
20.0	98.66	99.29
30.0	99.77	99.91
60.0	99.99	99.99

[a] The values in the table are percent dissolved.

isotropic behavior is given in Table II. The ratio of the time necessary for 50% dissolution is 1:1.97:2.69 for the profiles. For nonspherical single-particle dissolution, Pedersen and Brown (7) showed that spherical approximations give somewhat slower dissolution than the best approximations for fitting to the exact dissolution curves. The situation is also true in the dissolution of nonspherical powders.

Actually, acicular or flaky crystals do not grow isotropically, so they probably dissolve nonisotropically. The dissolution rate constant may be smaller for a larger side; *i.e.*, particles may dissolve faster from the smaller surface at the end of an acicular crystal (6). If it is assumed that three dissolution rate constants for rectangular parallelepipeds are proportional to the corresponding side lengths, as illustrated in Fig. 2, the particles are similar in shape throughout the dissolution. Then V_t in Eq. 1 can be written:

$$V_t = [a_0 - (2k_i/p)t][\alpha a_0 - (2k_i/p)t][\beta a_0 - (2k_i/p)t] \quad \text{(Eq. 9a)}$$

$$V_t = \alpha\beta[a_0 - (2k_i/p)t]^3 \quad \text{(Eq. 9b)}$$

In this case, $[1 + (1/\alpha) + (1/\beta)]$, $[(1/\alpha) + (1/\beta) + (1/\alpha\beta)]$, and $(1/\alpha\beta)$ in Eq. 5 are replaced by 3, 3, and 1, respectively. Hence, the final equation for S_T remains the same as the dissolution equation for the powder consisting of cubes or spheres.

In general, however, it is difficult to obtain the value of k_i; some average value is usually obtained, for example, by means of the disk method. The mean dissolution rate, k_{ia}, of three rates on the surface-area basis can be expressed by:

$$k_{ia} = \frac{(\alpha \times \beta)k_i + (1 \times \alpha)\beta k_i + (1 \times \beta)\alpha k_i}{(\alpha \times \beta) + (1 \times \alpha) + (1 \times \beta)} = \frac{3\alpha\beta}{\alpha\beta + \alpha + \beta} k_i \quad \text{(Eq. 10)}$$

The dissolution profile for needle-shaped particles (1 × 1 × 10 on the edges) with dissolution rate constants k_i, k_i, and $10k_i$ (M = 1.0, σ = 0.5, and p = 1.5) and the dissolution profile for these same particles with the

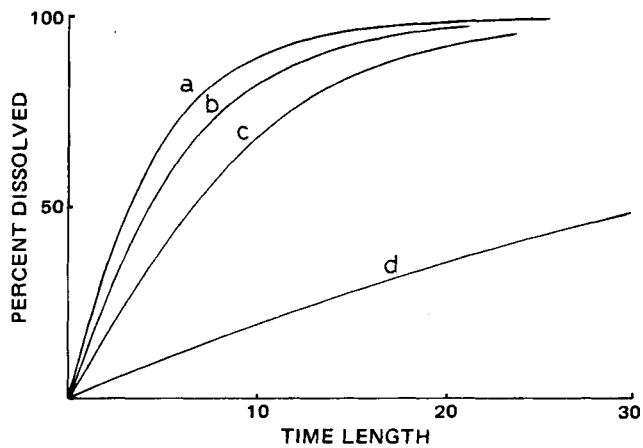

Figure 1—*Typical dissolution profiles for powders of cubic, acicular, and flaky particles with isotropic behavior. The constants used are* k_i *= 0.1,* M *= 1.0,* σ *= 0.5, and* p *= 1.5. Key: curve a, powder of cubic particles (1 × 1 × 1 on the edges); curve b, powder of acicular particles (1 × 1 × 10 on the edges); curve c, powder of flaky particles (1 × 10 × 10 on the edges); and curve d, powder of cubic particles (10 × 10 × 10 on the edges).*

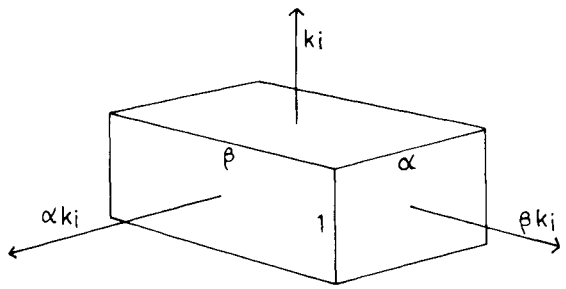

Figure 2—*Rectangular parallelepiped having the dissolution rate constants* k_i, αk_i, *and* βk_i.

average dissolution rate constant, k_{ia} ($M = 1.0$, $\sigma = 0.5$, $p = 1.5$, $\alpha = 1.0$, and $\beta = 10.0$), and with isotropic behavior are presented in Table III. Both profiles are almost the same. The ratio of the time necessary for 50% dissolution is 1:0.95. This result implies that the evaluation of the dissolution for the acicular or flaky particles with nonisotropic behavior is roughly possible by means of Eq. 6 using the mean dissolution rate constant, k_{ia}, which may be obtained experimentally as described.

The basic assumptions behind the theory are that the constituent particles are rectangular parallelepipeds that are similar in shape and dissolve isotropically under sink conditions. In actual situations, more factors may affect the overall dissolution profiles such as deviation from the log-normal law, irregularity in shape, and differences in the diffusion barrier for each particle, none of which is easily available. But these factors do not prevent an understanding of particle-shape effects on drug dissolution profiles, since they normally act independently of the effects.

In practical terms, the sizes of acicular or flaky particles measured microscopically or by an automated counter tend to be larger than those available for the evaluation of their dissolution profiles since the microscopic method does not always give the smallest side length but gives a larger one and the automated counter method gives volume diameter.

REFERENCES

(1) W. I. Higuchi and E. N. Hiestand, *J. Pharm. Sci.*, **52**, 67 (1963).

(2) W. I. Higuchi, E. L. Rowe, and E. N. Hiestand, *ibid.*, **52**, 162 (1963).

(3) D. Brooke, *ibid.*, **62**, 795 (1973).

(4) *Ibid.*, **63**, 344 (1974).

(5) P. V. Pedersen and K. F. Brown, *J. Pharm. Sci.*, **64**, 1192 (1975).

(6) J. T. Carstensen and M. Patel, *ibid.*, **64**, 1770 (1975).

(7) P. V. Pedersen and K. F. Brown, *ibid.*, **65**, 1437 (1976).

(8) "Handbook of Mathematical Functions with Formulas, Graphs, and Mathematical Tables," M. Abramowitz and I. A. Stegun, Eds., National Bureau of Standards, Washington, D.C., 1965.

Autoxidation of Polysorbates

M. DONBROW ˣ, E. AZAZ, and A. PILLERSDORF

Received September 6, 1977, from the *Pharmacy Department, School of Pharmacy, Hebrew University, Jerusalem, Israel.* Accepted for publication March 31, 1978.

Abstract □ Aqueous solutions of polysorbate 20 undergo autoxidation on storage, with the peroxide number increasing and subsequently decreasing again, the acidity increasing continuously, the pH and surface tension falling and tending to level off, and the cloud point dropping sharply until turbidity begins at room temperature. The changes are accelerated by light, elevation of temperature, and a copper sulfate catalyst. At the same time, hydrolysis occurs, liberating lauric acid. Analysis of the alterations in these properties leads to the conclusion that hydrolysis has the major influence near room temperature and that oxyethylene undergoes chain shortening at temperatures above 40°. However, evidence of degradation is detectable even in previously unopened commercial samples of polysorbates 20, 40, and 60, warranting attention to the stability of and standards for these surfactants as compared with the solid alkyl ether type of nonionic surfactant.

Keyphrases □ Polysorbates, various—autoxidation on storage, effect of light, temperature, and copper sulfate □ Oxidation—various polysorbates on storage, effect of light, temperature, and copper sulfate □ Stability—various polysorbates, autoxidation on storage, effect of light, temperature, and copper sulfate □ Degradation—various polysorbates, autoxidation on storage, effect of light, temperature, and copper sulfate □ Surfactants—various polysorbates, autoxidation on storage, effect of light, temperature, and copper sulfate

In view of accumulating evidence of the ease of autoxidation of polyethylene glycols and polyoxyethylene fatty alcohol ethers (1–4), it was suspected that other nonionic surfactants might undergo a similar process. Information about such reactions could increase the understanding of drug instability in aqueous solutions containing nonionic surfactants (1, 3).

The only systematic investigation of autoxidation in nonionic surfactants was carried out on cetomacrogol (1, 2). Peroxides were formed and decomposed spontaneously at rates increasing with temperature and decreasing with surfactant concentration. Furthermore, the induction period for peroxide chain propagation was shortened by an increase of temperature, a reduction of pH, a copper sulfate catalyst. The period was also reduced by the addition of chemical initiators, such as hydrogen peroxide or partially oxidized surfactant, and by free radical-initiating processes, such as exposure to light or thermal treatment as in sterilization by autoclaving.

During storage, the pH and cloud point fell and the acid content rose while the surface tension characteristics changed drastically. Polyglycols exhibited parallel changes in peroxide and acid content and in pH after autoclaving. These changes were interpreted as showing that degradation occurred in the hydrophilic chain with progressive reduction of the oxyethylene content until the hydrophilic–lipophilic balance fell below the critical value for solubility in water, when phase separation of the surfactant occurred at room temperature.

Since sorbitan derivatives are used widely, knowledge of their stability is important. Their behavior relative to the fatty alcohol ether type of surfactant may govern the choice between these two agents in a formulation. In the present work, the decomposition of polysorbate 20 (polyoxyethylene 20 sorbitan monolaurate) was studied systematically at controlled temperatures. The results are also

0022-3549/78/1200-1676$01.00/0